Available online at www.sciencedirect.com
SCIENCE DIRECT
Carbohydrate Polymers 64 (2006) 444–451
Carbohydrate Polymers
www.elsevier.com/locate/carbpol

X-ray diffraction study of crystal transformations in spherulitic amylose/lipid complexes from jet-cooked starch ☆

Randal L. Shogren [a,*], George F. Fanta [a,b], Frederick C. Felker [a,b]

[a] Plant Polymer Unit, National Center for Agricultural Utilization Research, USDA/ARS, 1815 N. University Street, Peoria, IL 61604, USA
[b] Cereal Products and Food Science Units, National Center for Agricultural Utilization Research, USDA/ARS, 1815 N. University Street, Peoria, IL 61604, USA

Received 9 September 2005; received in revised form 7 December 2005; accepted 13 December 2005
Available online 20 January 2006

Abstract

The effects of drying, solvent extraction and re-hydration on the structures of V-type amylose/lipid complexes from slowly cooled jet-cooked cornstarch dispersions were investigated using X-ray powder diffraction. Large spherulites in the wet state or dried in humid air had X-ray patterns similar to those found previously for wet amylose–isopropanol complexes (7_1 helices in orthorhombic unit cell). After freeze-drying, the X-ray pattern changed to a more disordered hexagonal array of 7_1 helices. Surprisingly, re-hydration in water caused a change to the 6_1 orthorhombic structure and then to the 6_1 hexagonal structure after a second freeze-drying. Extraction of the freeze-dried 7_1 forms with boiling anhydrous propanol did not change the diffraction pattern significantly but resulted in extraction of half of the complexed lipids. Extraction with boiling *n*-propanol/water resulted in complete lipid extraction along with conversion to the hexagonal V_6 form. The diffraction patterns of small particle amylose–lipid complexes (V_6) were unaffected by either re-hydration with water or extraction with alcohol or alcohol/water mixtures. Small angle X-ray scattering curves show small peaks at $d = 70$–80 Å, suggesting the presence of chain-folded crystallites.
Published by Elsevier Ltd.

Keywords: Starch; Complex; Spherulite; Diffraction; Fatty acid

1. Introduction

Amylose forms inclusion complexes with a wide variety of different organic and inorganic molecules (French & Murphy, 1977; Zobel, 1988). The guest molecules are thought to occupy the interior of a left-handed amylose helix which can have 6, 7 or 8 glucose residues per turn and a repeat distance of 8 Å. Thus, helix diameters increase with the number of glucose residues per turn and larger guest molecules can be accommodated. For example, 6_1 helices are formed from complexes of amylose with butanol and other linear alcohols (Rundle & Edwards, 1943; Yamashita, 1965; Yamashita, Ryugo, & Monobe, 1973) and fatty acids having 2 and >6 carbons, including the unsaturated acids oleic and linoleic (Takeo, Tokumura, & Kuge, 1973). Larger 7_1 helices are formed from amylose and branched alcohols such as tert-butanol, isopropanol, isobutanol (Yamashita & Hirai, 1966) as well as with butyric and valeric acids (Takeo et al., 1973). The even larger 8_1 helices are typically formed from amylose and napthol (Yamashita & Monobe, 1971). Detailed, atomic level structures derived from analyses of diffraction intensities have been presented for 6_1 crystalline complexes (Rappenecker & Zugenmaier, 1981; Winter & Sarko, 1974a,b; Zugenmaier & Sarko, 1976) and a preliminary structure for an 8_1 complex (Winter, Chanzy, Putaux, & Helbert, 1998). The former studies demonstrated hydrogen bonds between $O(2)_i$ and $O(3)_{i+1}$ (adjacent glucose residues) and between $O(6)_i$ and $O(2)_{i+6}$ (glucose residues on next turn). Complexes having the 7_1 helical conformation are presumed to exist from unit cell geometries derived from electron and X-ray diffraction data (Yamashita & Hirai, 1966).

The stability of crystalline amylose–guest V_6 complexes seems to depend on the size, hydrophility and amount of guest as well as moisture content. Solid state NMR studies have shown that amylose–acetic acid (Shogren, 2000) and amylose–butanol (Kawada & Marchessault, 2004) complexes are stable under vacuum conditions or heating to 90 °C, implying strong interactions, such as hydrogen bonding

☆ Names are necessary to report factually on available data; however, the USDA neither guarantees nor warrants the standard of the product and the use of the name by the USDA implies no approval of the product to the exclusion of others that may be suitable.

* Corresponding author. Tel.: +1 309 681 6354; fax: +1 309 681 6691.
E-mail address: shogrerl@ncaur.usda.gov (R.L. Shogren).

0144-8617/$ - see front matter Published by Elsevier Ltd.
doi:10.1016/j.carbpol.2005.12.018

between the guest and amylose. Upon humidification to 100% r.h., amylose complexed with small molecules such as small alcohols or DMSO changes to the B form while amylose complexed with large fatty acids such as lauric acid remains in the V_6 form (Kawada & Marchessault, 2004; Le Bail, Bizot, Pontoire, & Buleon, 1995; Saito, Yamada, Yukumoto, Yajima, & Ryuichi, 1991). Similarly, amylose–butanol complexes are soluble in water whereas amylose–fatty acid complexes are generally insoluble even in hot water (Zobel, 1988). Presumably, the increase in free energy associated with moving the hydrophobic fatty acid into an aqueous environment is large enough to prevent dissolution of the complex. Fatty acids can be extracted from amylose V_6 complexes with boiling alcohol and alcohol/water mixtures (Morrison & Coventry, 1989). Melting temperatures which reflect stability of water-swollen amylose–fatty acid complexes, as measured by DSC, tend to increase with fatty acid chain length, saturation and annealing (Karkalas, Ma, Morrison, & Pethrick, 1995; Raphaelides & Karkalas, 1988). There has been little work concerning the stability of 7_1 and 8_1 amylose helices with the exception of some reports of the transition of the 7_1 amylose–isopropanol complex to 6_1 on exposure to methanol (Buleon, Delage, Brisson, & Chanzy, 1990; Takeo & Kuge, 1969; Yamashita & Hirai, 1966) and transition of amylose–menthone complexes to 6_1 on exposure to ethanol (Rondeau-Mouro, Le Bail, & Buleon, 2004).

Recent work by Fanta, Felker, and Shogren (2002) has shown that two distinct types of spherulitic amylose–lipid crystals form on slow cooling of jet-cooked starch solutions. Typically >90% of these spherulites are large spherical/lobed particles consisting of 7_1 helices with the remainder being smaller torus-shaped spherulites consisting of 6_1 helices. This was the first report of amylose complexed with native lipids adopting the 7_1 conformation. Peterson, Fanta, Adlof, and Felker (2005) recently found that large and small spherulites contained the same types of complexed fatty acids and lysophopholipids but that the large 7_1 crystals were relatively enriched in linoleic acid while the smaller 6_1 crystals were enriched with palmitic acid. The large spherulites also formed first (at higher temperatures) followed by the small spherulites at lower temperatures.

In the course of our investigations, we have observed that the conformation of the spherical/lobed spherulites rapidly changed from 7_1 to 6_1 when spherulites that were originally isolated by freeze-drying were re-dispersed in water. This study was, therefore, carried out to better understand the stability of the 7_1 and 6_1 amylose–fatty acid spherulite forms under different solvent and hydration conditions. This information should be helpful in understanding the physical properties of starches in food systems as well as determining the stability of the spherulites under conditions, which might be encountered in possible practical applications such as adsorbents, chiral chromatography and catalyst supports.

2. Materials and methods

2.1. Materials

Unmodified, food grade cornstarch was a product of A.E. Staley Mfg. Co., Decatur, IL. High amylose cornstarch (Amylomaize VII) was a product of Cerestar, Hammond, IN. *n*-propanol (99+%, spectrophotometric grade), 2-propanol (99.5%, HPLC grade), and ethanol (99.5%, ACS reagent) were purchased from Sigma–Aldrich. Methanol (HPLC grade) and acetone (HPLC grade) were purchased from Fisher Scientific.

2.2. Jet cooking of starch and isolation of spherocrystalline material

Large spherical, lobed particles and smaller torus shaped particles were prepared from normal and high amylose starches as described previously (Fanta et al., 2002). Spherulites were fractionated according to particle size by allowing dilute water dipersions to partially settle, leaving the smaller particles in suspension. The efficiency of this fractionation procedure was monitored by light microscopy.

2.3. X-ray diffraction

X-ray powder diffraction was carried out in reflection mode as described previously (Fanta, Shogren, & Salch, 1999) using a Philips PW1820/1830 goniometer/generator (PANalytical, Bollingbrook, IL) and Cu K_α. (1.54178 Å) radiation. Briefly, powder samples were scanned from 3 to 30° 2θ in 0.05° steps at 8 s per step. Unless stated otherwise, freeze-dried spherulite samples were equilibrated at 23 °C and 50% r.h. for 2 days prior to analysis. Wet starch samples were scanned at 32 s per 0.05° step to increase scattered intensity. A small pan of water was placed in the sample compartment with the wet samples to prevent drying. Low angle X-ray scattering measurements were carried out using a Bruker NanoStar system (Bruker AXS Inc., Madison, WI) using Cu K_α radiation and position sensitive area detector. Freeze-dried powder samples were mounted between two pieces of Scotch tape. Scattering from the tape was subtracted from the sample data. A sample of silver behenate was used to calibrate sample–detector distance and corrections for sample transmission using the 'indirect' method were made using a strong scattering standard (glassy carbon).

2.4. Nuclear magnetic resonance

CP/MAS C-13 NMR spectra were obtained using a Bruker MSL-300 spectrometer. Samples were spun in zirconia rotors at 3–4000 Hz. Pulse widths, mix times and delay times were 5 μs, 2 ms and 5 s, respectively.

3. Results

Fig. 1 shows diffraction patterns of the large spherical/lobed and small torus-shaped amylose–lipid spherulites in the

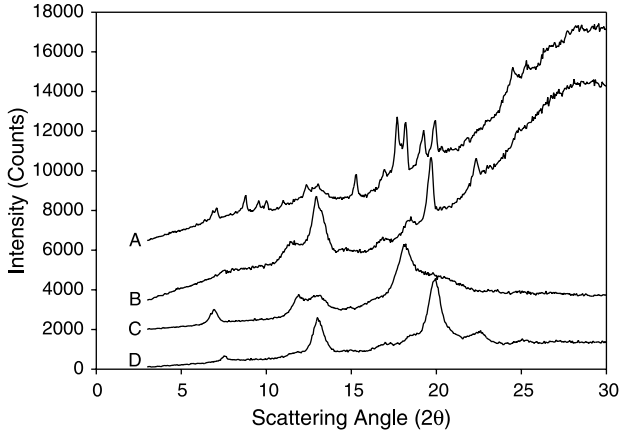

Fig. 1. X-ray diffraction of wet, never dried large (A) and small (B) starch spherulites; and freeze-dried large (C) and small (D) spherulites.

wet state (never dried) and after freeze-drying. The pattern for the wet, large spherulites (Fig. 1(A)) has numerous sharp reflections and is similar to the results of Yamashita and Hirai (1966) for wet amylose–isopropanol V_7 crystals. Scattering angles of major reflections for our data and Yamashita and Hirai (1966) are compared in Table 1 and appear quite similar. They proposed an orthorhombic unit cell consisting of four chains each with seven residues per turn and 15.0 Å in diameter. After freeze-drying (Fig. 1(C)), three rather broad peaks at $2\theta = 7.0$, 11.9 and 18.1° are evident, consistent with a transition to a less ordered, hexagonal unit cell having V_7 helical chains 14.7 Å in diameter (Yamashita & Hirai, 1966). Thus, water is important in stabilizing intermolecular interactions in these V_7 amylose–lipid crystals. As summarized by French and Murphy (1977), water and sometimes complexing agents may occupy spaces between amylose helices thus expanding the unit cell and changing it's geometry. Indeed, Winter and Sarko (1974a,b) have suggested, based on a detailed X-ray diffraction study, that some water molecules form hydrogen bonds between adjacent 6_1 helices in the orthorhombic unit cell of V-anhydrous amylose, thus stabilizing the structure. The X-ray diffraction pattern for both the wet (Fig. 1(B)) and dry (Fig. 1(D)) small amylose–lipid crystals were similar and had three reflections at 7.5, 13.0, 19.9° 2θ, typical of 6_1 helical chains in a hexagonal unit cell (Table 1).

Fig. 2 shows X-ray diffraction patterns of large spherulites dried at 50% relative humidity and then ground to a powder. The pattern for the powder sample is similar to the wet form (orthorhombic V_7) though reflections are somewhat broader, suggesting some loss in order.

Fig. 3 shows X-ray diffraction patterns of large and small spherulites after rewetting of the freeze-dried samples with water and then isolating the spherulites once again by freeze-drying. The rewet but undried large amylose–lipid spherulites (Fig. 3(A)) have an X-ray pattern similar to that found for wet amylose–*n*-butanol complexes (Table 1) (Yamashita, 1965). The latter were indexed to a orthorhombic unit cell with 6_1 amylose helices having diameter of 13.7 Å. After the rewet spherulites were once again freeze-dried, three reflections having $2\theta = 7.50$, 12.8 and 19.9° were seen (Fig. 3(C)) which is typical of 6_1 amylose complexes in a hexagonal unit cell. Rewetting with water thus causes the transition from V_7 to V_6 helical conformation to take place in the freeze-dried large spherulites. Therefore, it would seem that the V_6 helix is the more stable, lower energy form under room temperature conditions. There was little change in the X-ray patterns of the small particle spherulites after rewetting and freeze-drying (compare Fig. 3(B) and (D) with Fig. 1(B) and (D)).

Fig. 4 shows phase-contrast optical micrographs of large spherulites in freshly made aqueous suspension (Fig. 4(A)) and after freeze-drying and then rehydrating (Fig. 4(B)). After rehydration, spherulites were slightly smaller and there was less contrast between the darker interior and lighter exterior. These changes may have resulted from shrinkage during drying. Overall, the difference in appearance is rather small, suggesting that the conformational transition from V_7 to V_6 does not change the gross morphology of the spherulitic crystals. When viewed with crossed polarizers (not shown), both samples

Table 1
Scattering angles (degrees 2θ) for major reflections of large spherulites compared with literature data for V7 and V6 complexes

Wet (Fig. 1(A))	Wet V7[a]	F-D (Fig. 1(C))	Dry V7[b]	F–D rewet (Fig. 3(A))	Wet V6[c]	F–D, rewet, F–D (Fig. 3(C))	Dry V6[d]
7.1	7.0	7.0	7.2	9.5	9.3	7.6	7.5
8.8	8.8	11.9	12.3	12.1	11.8	12.9	12.9
9.5	9.7	13.2	13.3	13.3	12.8	19.9	20.0
10.0		18.1	18.6	20.1	19.8		
12.4	12.8			21.3	21.0		
13.0							
15.3	15.3						
17.7	18.0						
18.2							
19.3	19.2						
19.9	20.0						
24.5	24.7						
25.3							

[a] Data for moist amylose–isopropanol complex, from Yamashita and Hirai (1966).
[b] Data for dried (100 °C, vacuo) amylose–isopropanol complex, from Yamashita and Hirai (1966).
[c] Data for moist amylose–butanol complex, from Yamashita (1965).
[d] Data for dried (in dessicator) amylose–butanol complex, from Yamashita (1965).

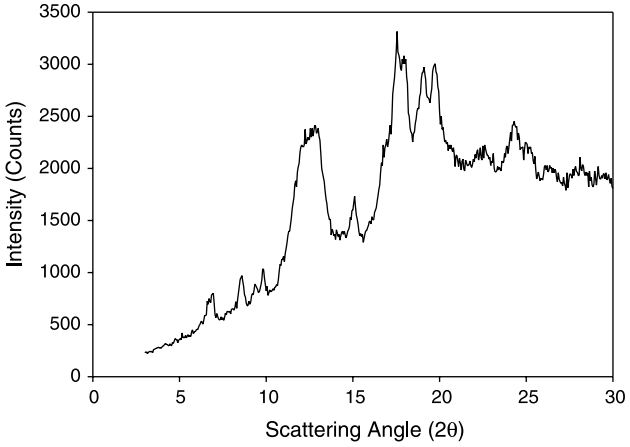

Fig. 2. X-ray diffraction of large spherulites dried at 50% r.h. after grinding into a powder with a mortar and pestle.

showed the characteristic banded birefringence pattern described previously (Fanta et al., 2002), suggesting similar orientation of molecules within the crystals.

Fig. 5 shows X-ray diffraction patterns of large spherical/lobed spherulites before extraction (Fig. 5(A)) and after extraction with boiling *n*-propanol/water 75/25 for 2 h (Fig. 5(D)), with *n*-propanol/water 75/25 for 2 h at room temperature (Fig. 5(C)) and with pure, boiling *n*-propanol (no water) for 2 h (Fig. 5(B)). Extracted samples were allowed to air dry under ambient conditions. Irrespective of extraction temperature, large spherocrystals extracted with *n*-propanol/water 75/25 are converted from the V_7 to V_6 form. The V_7 pattern is, however, largely retained after extraction with hot *n*-propanol alone. The presence of water is thus required for the V_7 to V_6 transition to occur. The V_7 to V_6 transition was also found to occur after room temperature extraction with ethanol/water 3/1, methanol/water 3/1, acetone/water 3/1, isopropanol/water 3/1 and pure water alone (X-ray patterns not shown).

Solid state, CP/MAS ^{13}C NMR spectra for selected solvent extracted large spherical/lobed spherulites are shown in Fig. 6.

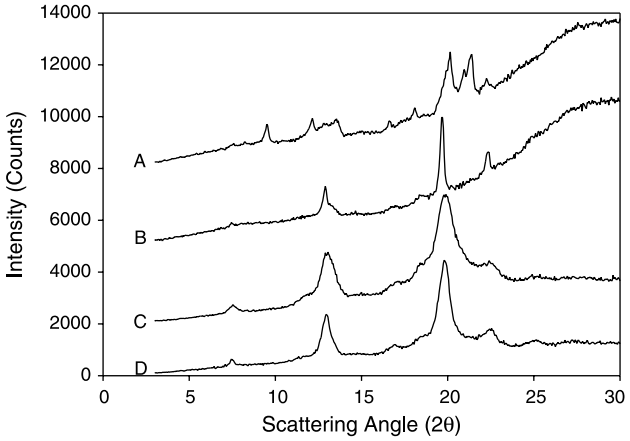

Fig. 3. X-ray diffraction of large (A) and small (B) spherulites after freeze-drying and rewetting; and large (C) and small (D) spherulites after second freeze-drying.

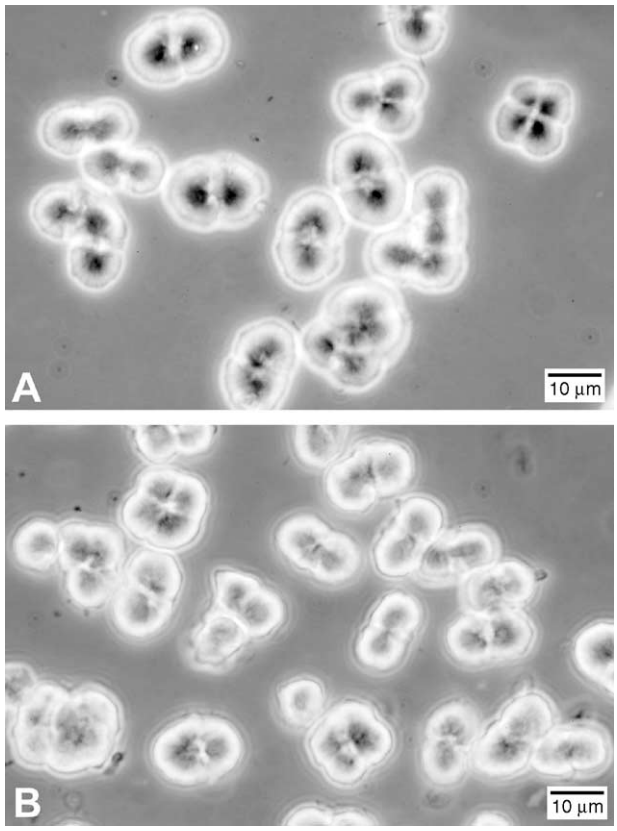

Fig. 4. Phase-contrast optical micrographs of wet, never dried large spherulites (A) and after freeze-drying and re-hydration (B).

Lipid CH_2 and CH_3 resonances are apparent at 25–35 ppm and 15 ppm, respectively, while starch CH resonances are apparent at 60–85 ppm (C2–C6) and 95–108 ppm (C1). Spinning side bands of the starch resonances overlap some of the CH_2 resonances as indicated by the arrows. Therefore, ratios of

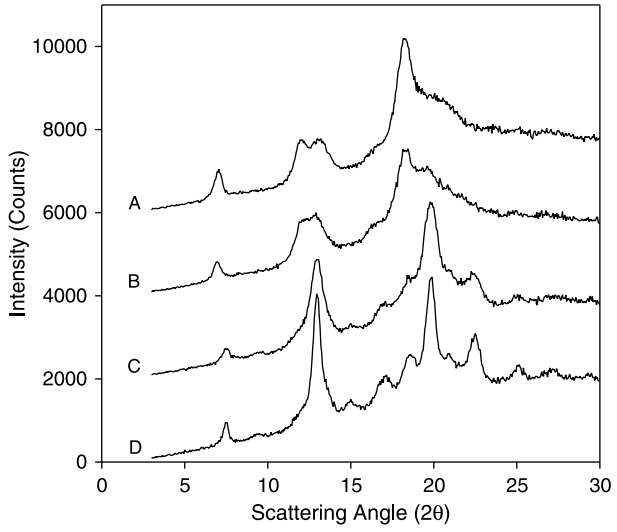

Fig. 5. X-ray diffraction of freeze-dried large spherulites (A), after extraction with boiling *n*-propanol (B), after extraction with *n*-propanol/water at room temperature (C) and after extraction with boiling *n*-propanol/water (D).

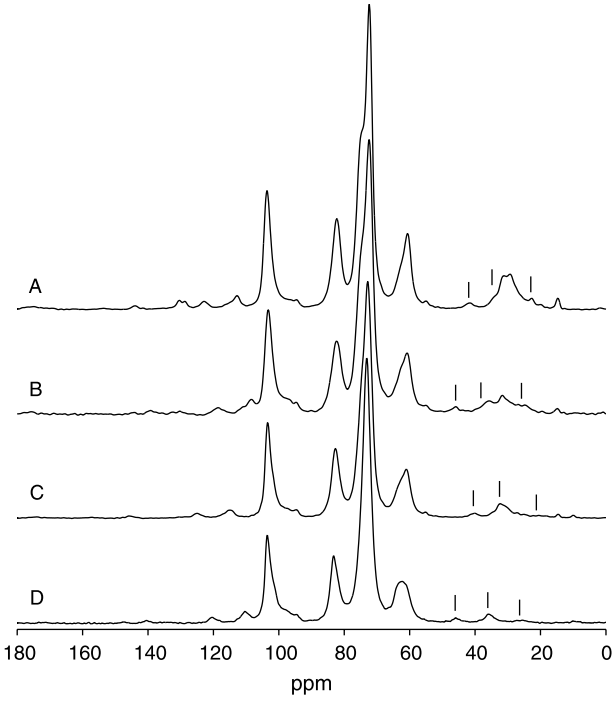

Fig. 6. CP/MAS ^{13}C NMR spectra for freeze-dried large spherulites (A), after extraction with boiling *n*-propanol (B), after extraction with *n*-propanol/water at room temperature (C) and after extraction with boiling *n*-propanol/water (D). Small vertical lines indicate spinning side bands.

lipid/starch by weight were estimated from the ratio of areas of the lipid CH_3 resonance to the starch C1 resonance:

$$\frac{\text{Weight lipid}}{\text{Weight starch}} = \frac{A(CH_3)}{A(C1)}\frac{284}{162} \quad (1)$$

where the molecular weight of stearic acid (284) was used to approximate the molecular weight of lipid and *A* is the area of the respective peaks. The resulting ratios were 0.073, 0.038, 0.016 and 0 for large spherulites before extraction, after extraction with boiling neat *n*-propanol, *n*-propanol/water at room temperature and boiling *n*-propanol/water, respectively. These results confirm that *n*-propanol and *n*-propanol–water mixtures do indeed extract much or all of the lipids from crystalline amylose complexes in the V_7 form. In agreement with Morrison and Coventry (1989), refluxing 75/25 *n*-propanol/water is the most efficient solvent system for lipid extraction. These data and the X-ray and microscopy data shown earlier also indicate that amylose retains its crystalline, helical form after lipids are removed so an array of 'hollow' helical 'nanotubes' is left. It was observed that after solvent extraction, the spherulites swell and appear to solubilize when placed in water.

Small angle X-ray scattering (SAXS) curves for freeze-dried large spherical/lobed spherulites, small toroidal spherulites and native cornstarch are shown in Fig. 7. Small peaks appeared at scattering vectors $q = 0.08$–0.09 Å^{-1} which corresponds to spacings of $d = 70$–80 Å. These spacings are similar to values of approximately 90 Å found previously for native cornstarch (Sterling, 1962; Tester, Karkalas, & Qi, 2004) and correspond to a regular, repeating structure of crystalline and amorphous regions.

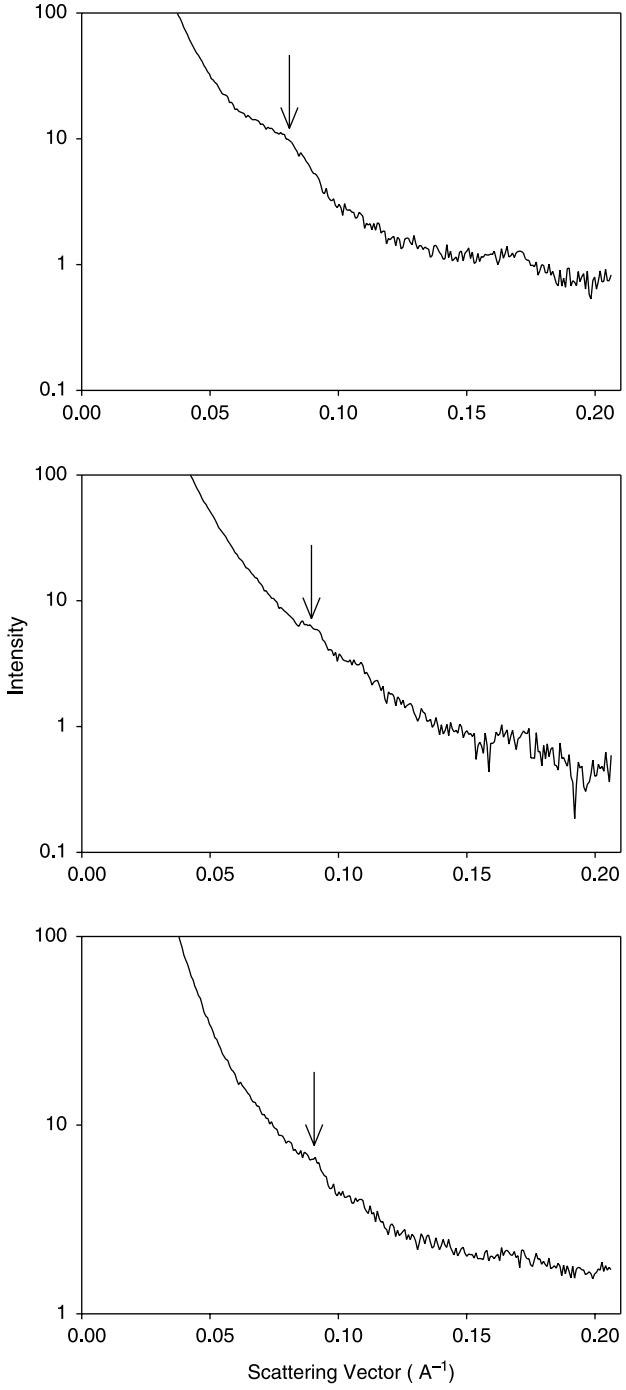

Fig. 7. Small angle X-ray scattering (SAXS) curves for large spherulites (A), small toroidal crystals (B) and native cornstarch (C).

4. Discussion and conclusions

Spherulites are formed from helical inclusion complexes of amylose with the native lipids normally present in minor amounts in cereal starch granules. In cornstarch, this native lipid fraction is comprised largely of fatty acids, the major components being palmitic acid and linoleic acid. Previous studies of amylose–guest complexes by electron microscopy and diffraction have demonstrated that these complexes form lamellar single crystals approximately 100 Å thick with the

amylose chains perpendicular to the crystal surface in a chain-folded configuration (Yamashita et al., 1973). Thus, the large spherical/lobed and the small torus-shaped spherulites likely consist of layers of chain-folded amylose–lipid helices (i.e. crystalline lamellae) about 80 Å in thickness with the helices oriented radially. The latter supposition is supported by the banded maltese cross pattern of birefringence noted earlier for the spherical/lobed species (Fanta et al., 2002).

The morphology of spherulites has been ascribed to branching of lamellae and also to imperfect stacking of individual lamellae during the growth process due to repulsive forces caused by portions of un-crystallized polymer chains that are not chain-folded and thus extend from lamella surfaces (Abo el Maaty, Hosier, & Bassett, 1998; Bassett, 1999). It is interesting that electron micrographs of polyolefin spherulites (Bassett, 1984) resembled the structures of the amylose/lipid spherulites observed in this study. Also, Kalinka and Hinrichsen (1997) have published computer simulations of spherulite growth from crystalline lamellae and have considered the effects of several variables on spherulite morphology. Even though these authors made no specific mention of the amylose/lipid system, their computer-simulated structures were also similar to the structures actually observed for our spherical/lobed particles.

Crystal transformations of the large spherical/lobed spherulites are summarized schematically in Fig. 8. The facile conformational change from V_7 to V_6 was unexpected, and it is clear that this transition is caused by the presence of water. Although it is well known that aqueous alcohols, particularly 75/25 *n*-propanol/water, will extract complexed native lipids from amylose (Morrison & Coventry, 1989), the extraction of native lipid from the amylose helix and replacing it with *n*-propanol is not necessary for the transition to take place since the conformational change takes place in water alone at room temperature. Fatty acids can be partially or fully extracted from both the large and small spherulite species with retention of the V helical structure, leaving an array of 'nanotubes'. The fact that spherulite morphology is not appreciably changed by the V_7 to V_6 transition is not surprising, since formation and stacking of individual crystalline lamellae to form the individual spherulites occurs when hot, jet-cooked dispersions are cooled. Once formed, spherulites are not likely to change in outward appearance unless they are re-heated in water. Also, molecular modeling suggests that the change in glycosidic torsional angles $\emptyset$, Φ accompanying the V_7 to V_6 transition is rather small ($-18°$, $-3°$ for V_7; $-14°$, $-6°$ for V_6) (French & Murphy, 1977).

If amylose complexes are formed from fatty acids that exist as dimers during steam jet cooking (as opposed to single molecules of dissolved fatty acid), an explanation can be proposed for the conformational transition from 7_1V to 6_1V when freeze-dried spherical/lobed spherulites are placed back into an aqueous environment. The formation of fatty acid dimers (or higher order structures such as trimers, etc.) is likely because of the low solubility of these fatty acids in water, despite the high temperature/high shear conditions of the steam jet cooking process. Formation of dimeric structures (A) and (B) in Fig. 9 would minimize the unfavorable energy associated with the interaction of individual aliphatic chains with water. This type of association of alkyl chains has been referred to as hydrophobic bonding or interaction (Mukerjee, 1965; Némethy, 1967; Schrier, Pottle, & Scheraga, 1964; Yamamoto & Nishi, 1990). The bulky nature of these dimeric structures would cause the amylose helix to assume the 7_1V conformation, and the low temperature of the freeze-drying process would keep water molecules frozen, thus eliminating the plasticizing effect of water during drying and causing the 7_1V conformation to be maintained during the drying process. After the water is removed by freeze-drying, dimer structures (A) and (B) would be less energetically favorable; and the dimer within the dried amylose helix would rearrange to the less sterically hindered structure (C). In the absence of water, structure (C) would be of lower energy due to hydrogen bonding between carboxyl substituents. When the freeze-dried

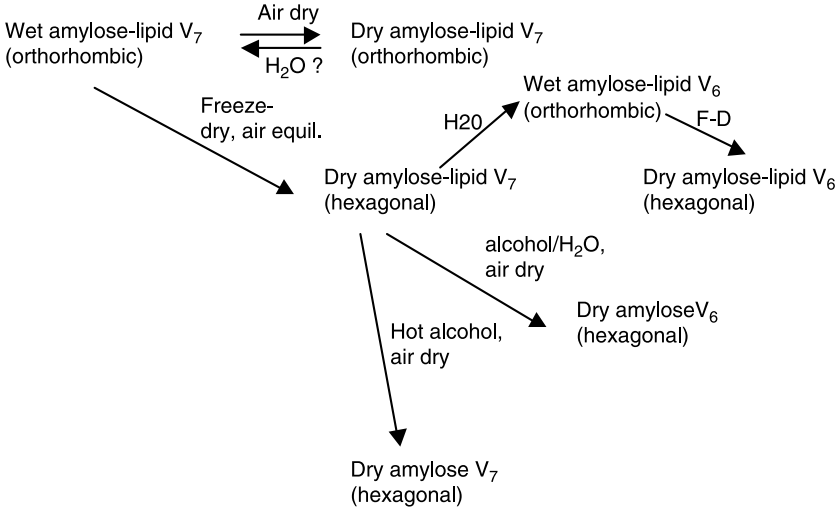

Fig. 8. Diagram of changes in crystal structure of large spherulites with drying, re-hydration and solvent extraction.

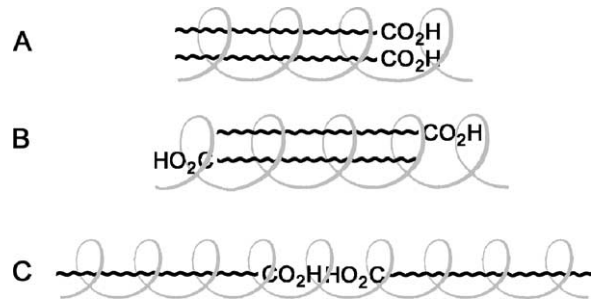

Fig. 9. Schematic diagram of hypothesized changes in fatty acid association in amylose complexes: side-by-side dimers (or multimers) in the wet, never dried V_7 large spherulites (A, B); linear arrangement of fatty acids after freeze-drying (V_6).

spherulites are placed back into an aqueous environment, water will plasticize the amylose helix; and if the bulky dimeric structures (A) and (B) are not present to force the helix into the 7_1V conformation, the plasticized helix will revert to the more thermodynamically stable 6_1V form. Further work will be necessary to validate this theory.

Several authors have suggested that, based on molecular modeling and NMR relaxation data that the carboxyl group of fatty acids must be located outside the amylose V helix (Godet, Buleon, Tran, & Colonna, 1993a; Godet, Tran, Delage, & Buleon, 1993b; Kawada & Marchessault, 2004; Lebail, Buleon, Shiftan, & Marchessault, 2000; Snape, Morrison, Maroto-Valer, Karkalas, & Pethrick, 1998). The finding of large (70–100 Å) thick crystalline lamellae argues against this hypothesis since 4–6 fatty acid molecules would be needed to span that length and any bulky carboxyl groups protruding outside the helices would be expected to disrupt chain packing. Upfield shifts of the carboxyl NMR resonances in amylose complexes (Shogren, 2000; Shogren, Thompson, Greene, Gordon, & Cote, 1991) as well as the formation of highly crystalline amylose complexes with fatty acids as small as acetic acid (Shogren, 2000; Takeo et al., 1973) further support the idea that carboxyl groups are located inside the amylose helix.

Acknowledgements

The authors would like to thank Dr Arthur Thompson for the NMR experiments and Bruker AXS for the SAXS experiments.

References

Abo el Maaty, M. I., Hosier, I. L., & Bassett, D. C. (1998). A unified context for spherulite growth in polymers. *Macromolecules*, *31*, 153–157.

Bassett, D. C. (1984). *Electron microscopy and spherulitic organization in polymers CRC critical reviews in solid state and materials science*. *Vol. 12* pp. 97–163. *Cleveland, OH*: *CRC Press* (Issue 2).

Bassett, D. C. (1999). On spherulite growth and cellulation in polymers. A unified context. *Polymer Journal*, *31*, 759–764.

Buleon, A., Delage, M. M., Brisson, J., & Chanzy, H. (1990). Single crystals of V amylose complexed with isopropanol and acetone. *International Journal of Biological Macromolecules*, *12*, 25–33.

Fanta, G. F., Felker, F. C., & Shogren, R. L. (2002). Formation of crystalline aggregates in slowly-cooled starch solutions prepared by steam jet cooking. *Carbohydrate Polymers*, *48*, 161–170.

Fanta, G. F., Shogren, R. L., & Salch, J. H. (1999). Steam jet cooking of high amylose starch–fatty acid mixtures. An investigation of complex formation. *Carbohydrate Polymers*, *38*, 1–6.

French, A. D., & Murphy, V. G. (1977). Computer modeling in the study of starch. *Cereal Foods World*, *22*, 61–70.

Godet, M. C., Buleon, A., Tran, V., & Colonna, P. (1993a). Structural features of fatty acid–amylose complexes. *Carbohydrate Polymers*, *21*, 91–95.

Godet, M. C., Tran, V., Delage, M. M., & Buleon, A. (1993b). Molecular modeling of the specific interactions involved in the amylose complexation by fatty acids. *International Journal of Biological Macromolecules*, *15*, 11–16.

Kalinka, G., & Hinrichsen, G. (1997). Two-dimensional computer simulation of spherulite formation by branching lamellae. *Acta Polymer*, 256–261.

Karkalas, J., Ma, S., Morrison, W. R., & Pethrick, R. A. (1995). Some factors determining the thermal properties of amylose inclusion complexes with fatty acids. *Carbohydrate Research*, *268*, 233–247.

Kawada, J., & Marchessault, R. H. (2004). Solid state NMR and X-ray studies on amylose complexes with small organic molecules. *Starch/Stärke*, *56*, 13–19.

Le Bail, P., Bizot, H., Pontoire, B., & Buleon, A. (1995). Polymorphic transitions of amylose–ethanol crystalline complexes induced by moisture exchanges. *Starch/Stärke*, *47*, 229–232.

Lebail, P., Buleon, A., Shiftan, D., & Marchessault, R. H. (2000). Mobility of lipid in complexes of amylose–fatty acids by deuterium and 13C solid state NMR. *Carbohydrate Polymers*, *43*, 317–326.

Morrison, W. R., & Coventry, A. M. (1989). Solvent extraction of fatty acids from amylose inclusion complexes. *Starch/Stärke*, *41*, 24–27.

Mukerjee, P. (1965). Dimerization of long-chain fatty acids in aqueous solutions and the hydrophobic properties of the acids. *Journal of Physical Chemistry*, *69*, 2821–2827.

Némethy, G. (1967). Hydrophobic interactions. *Angewandte Chemie, International Edition*, *6*, 195–280.

Peterson, S. C., Fanta, G. F., Adlof, R. O., & Felker, F. C. (2005). Identification of complexed native lipids in crystalline aggregates formed from jet cooked cornstarch. *Carbohydrate Polymers*, *61*, 162–167.

Raphaelides, S., & Karkalas, J. (1988). Thermal dissociation of amylose–fatty acid complexes. *Carbohydrate Research*, *172*, 65–82.

Rappenecker, G., & Zugenmaier, P. (1981). Detailed refinement of the crystal structure of V_h-amylose. *Carbohydrate Research*, *89*, 11–19.

Rondeau-Mouro, C., Le Bail, P., & Buleon, A. (2004). Structural investigation of amylose complexes with small ligands: Inter- or intra-helical associations? *International Journal of Biological Macromolecules*, *34*, 309–315.

Rundle, R. E., & Edwards, R. C. (1943). The configuration of starch in the starch–iodine complex IV. An X-ray diffraction investigation of butanol-precipitated amylose. *Journal of the American Chemical Society*, *65*, 2200–2203.

Saito, H., Yamada, J., Yukumoto, T., Yajima, H., & Ryuichi, E. (1991). Conformational stability of V-amyloses and their hydration-induced conversion to B-type form as studied by high resolution solid-state ^{13}C NMR spectroscopy. *Bulletin of the Chemical Society of Japan*, *64*, 3528–3537.

Schrier, E. E., Pottle, M., & Scheraga, H. A. (1964). The influence of hydrogen and hydrophobic bonds on the stability of the carboxylic acid dimers in aqueous solution. *Journal of the American Chemical Society*, *86*, 3444–3449.

Shogren, R. L. (2000). Modification of maize starch by thermal processing in glacial acetic acid. *Carbohydrate Polymers*, *43*, 309–315.

Shogren, R. L., Thompson, A. R., Greene, R. V., Gordon, S. H., & Cote, G. (1991). Complexes of starch polysaccharides and poly(ethylene *co*-acrylic acid): Structural characterization in the solid state. *Journal of Applied Polymer Science*, *42*, 2279–2286.

Snape, C. E., Morrison, W. R., Maroto-Valer, M., Karkalas, J., & Pethrick, R. A. (1998). Solid state 13C NMR investigation of lipid ligands in V-amylose inclusion complexes. *Carbohydrate Polymers*, *36*, 225–237.

Sterling, C. (1962). A low angle spacing in starch. *Journal of Polymer Science*, *56*, S10–S12.

Takeo, K., & Kuge, T. (1969). Complexes of starchy materials with organic compounds part III. X-ray studies on amylose and cyclodextrin complexes. *Agricultural and Biological Chemistry*, *33*, 1174–1180.

Takeo, K., Tokumura, A., & Kuge, T. (1973). Complexes of starch and its related materials with organic compounds. Part X. X-ray diffraction of amylose–fatty acid complexes. *Die Stärke*, *25*, 357–388.

Tester, R. F., Karkalas, J., & Qi, X. (2004). Starch–composition, fine structure and architecture. *Journal of Cereal Science*, *39*, 151–165.

Winter, W. T., Chanzy, H., Putaux, J., & Helbert, W. (1998). Inclusion compounds of amylose. *Polymer Preprints*, *39*, 703.

Winter, W. T., & Sarko, A. (1974a). Crystal and molecular structure of V-anyhydrous amylose. *Biopolymers*, *13*, 1447–1460.

Winter, W. T., & Sarko, A. (1974b). Crystal and molecular structure of the amylose–DMSO complex. *Biopolymers*, *13*, 1461–1482.

Yamamoto, K., & Nishi, N. (1990). Hydrophobic hydration and hydrophobic interaction of carboxylic acids in aqueous solution: Mass spectrometric analysis of liquid fragments isolated as clusters. *Journal of the American Chemical Society*, *112*, 549–558.

Yamashita, Y. (1965). Single crystals of amylose V complexes. *Journal of Polymer Science Part A*, *3*, 3251–3260.

Yamashita, Y., & Hirai, N. (1966). Single crystals of amylose V complexes. II. Crystals with 7_1 helical configuration. *Journal of Polymer Science Part A-2*, *4*, 161–171.

Yamashita, Y., & Monobe, K. (1971). Single crystals of amylose V complexes. III. Crystals with 8_1 helical configuration. *Journal of Polymer Science Part A-2*, *9*, 1471–1481.

Yamashita, Y., Ryugo, J., & Monobe, K. (1973). An electron microscopic study on crystals of amylose V complexes. *Journal of Electron Microscopy*, *22*, 19–26.

Zobel, H. F. (1988). Starch crystal transformations and their industrial importance. *Starch/Stärke*, *40*, 1–7.

Zugenmaier, P., & Sarko, A. (1976). Packing analysis of carbohydrates and polysaccharides. IV. A new method for detailed crystal structure refinement of polysaccharides and its application to V-amylose. *Biopolymers*, *15*, 2121–2136.